PHYSICAL REVIEW B **83**, 100101(R) (2011)

Optical anisotropy and charge-transfer transition energies in $BiFeO_3$ from 1.0 to 5.5 eV

S. G. Choi,[1,*] H. T. Yi,[2] S.-W. Cheong,[2] J. N. Hilfiker,[3] R. France,[1] and A. G. Norman[1]

[1]*National Renewable Energy Laboratory, Golden, Colorado 80401, USA*

[2]*Rutgers Center for Emergent Materials and Department of Electrical and Computer Engineering, Rutgers University, Piscataway, New Jersey 08854, USA*

[3]*J. A. Woollam Co. Inc., Lincoln, Nebraska 68508, USA*

(Received 29 December 2010; revised manuscript received 26 January 2011; published 30 March 2011)

We discuss uniaxial optical anisotropy in single-crystal $BiFeO_3$ determined by spectroscopic ellipsometry from 1.0 to 5.5 eV. The dielectric function $\varepsilon = \varepsilon_1 + i\varepsilon_2$ and refractive index $N = n + ik$ spectra of $BiFeO_3$ are extracted for the tensor components along its ordinary and extraordinary principal axes. Using the standard line-shape analysis, we also obtain the energies of the major optical structures associated with the charge-transfer transitions in $BiFeO_3$.

DOI: 10.1103/PhysRevB.83.100101 PACS number(s): 78.20.Ci, 07.60.Fs, 75.85.+t

Bismuth ferrite ($BiFeO_3$) is so far the only known compound that exhibits both antiferromagnetism and a strong ferroelectricity at room temperature.[1–3] Such a unique multiferroic characteristic has made $BiFeO_3$ a very attractive material for fundamental physics studies.[1–4] For practical applications,[3] possible electrical manipulation of the magnetic states (magnetoelectric coupling) has stimulated an intense effort to realize various devices in magnetoelectric memory storage and electric-field control of magnetic sensors, for example. Also, the large saturation polarization and the smaller bandgap (than many other ferroelectric perovskite compounds) of $BiFeO_3$ pave a new path toward oxide-based photovoltaic devices.[5,6]

Crystal $BiFeO_3$ forms in the *pseudocubic* rhombohedral structure belonging to the *R*3*c* space group, but the unit cell can also be described as the hexagonal structure with the *c* axis lying in the [111] axis of the *pseudocubic* reference frame.[3] The electric polarization vector $\vec{P}$ of this compound is also along [111]. Thus, the [111] axis is distinguished from the remaining three $\langle 111 \rangle$ axes. In the *pseudocubic* reference frame, there are six equivalent$\langle 1\bar{1}0 \rangle$ axes normal to the [111] direction that form a plane. Since a second-rank polarizability tensor cannot support a threefold rotational anisotropy, the optical properties are essentially the same for any polarization in this plane. Consequently, $BiFeO_3$ has uniaxial optical anisotropy with the optic axis along the [111] axis.

Spectroscopic ellipsometry (SE) is a highly suitable method of determining complex optical functions over a wide range of photon energy, and therefore, many interesting SE studies[7–9] have recently been performed on epitaxial $BiFeO_3$ thin films. However, no systematic SE study has yet been reported on the optical anisotropy in $BiFeO_3$. The mixed ferroelectric domain structures presented in thin films probably obscured the anisotropic nature of this crystal in previous SE work.[7]

Here, we apply SE to determine the ordinary and extraordinary components of the dielectric function $\varepsilon = \varepsilon_1 + i\varepsilon_2$ and refractive index $N = n + ik$ tensor for $BiFeO_3$. Our spectra exhibit distinct optical structures associated with the charge-transfer transitions. The energies of these transitions are accurately obtained by using the standard line-shape analysis.[10]

A single-domain $BiFeO_3$ bulk crystal was grown by the flux growth method where $Bi_2O_3/Fe_2O_3/B_2O_3$ were mixed and sintered at around 870 °C. The as-grown crystal was first cut and polished, followed by a dilute nitric acid etch and a 10-h anneal at 300 °C in argon to relieve any strain from the polishing. This procedure left a platelet with facets normal to [001] larger than 1 mm^2. The formation of a single domain structure was explicitly verified using polarized optical microscopy. Additional details of the growth and structural characterization can be found in Ref. 5.

Generalized variable-angle SE (g-VASE) measurements[11] were performed with the sample at room temperature from 1.0 to 5.5 eV using a rotating compensator-type SE (M2000-DI model, J. A. Woollam Inc.) equipped with a manual *in-plane* rotation sample stage. Data were recorded at multiple crystallographic orientations by rotating the sample about the surface normal in steps of 15°. The incident angle of the probing light was also varied from 45° to 75° with an increment of 15° per orientation.

We reduced the surface overlayer artifacts[12] in the SE data to the maximum extent possible by polishing the surface using a colloidal silica suspension with 0.02-μm particles, followed by deionized water, acetone, and methanol rinses. Immediately prior to the SE measurements, we further cleaned the surface for 20 min in an ultraviolet (UV) ozone cleaner. This UV ozone cleaning procedure has been proven to effectively remove carbon-related contaminants from the surface of oxide compounds.[13] Nitrogen gas was continuously flowed onto the sample during the measurements to minimize the possible recontamination of the surface.

Fugures 1(a) and 1(b) show the real and imaginary parts of the *pseudodielectric function* $\langle \varepsilon \rangle = \langle \varepsilon_1 \rangle + i\langle \varepsilon_2 \rangle$ spectra, respectively, recorded at an incident angle of 75° along four different crystallographic orientations: [100], [110], [010], and [$\bar{1}$10]. The crystal orientations were determined by measuring the unique Bragg angles of the four asymmetric {113} planes using high-resolution x-ray diffraction. Two pronounced optical structures at around 3 and 4 eV with a small shoulder at ~2.5 eV are commonly seen from all the spectra. Our $\langle \varepsilon_2 \rangle$ spectra reveal that the optical structure at ~4 eV has two contributions that vary in relative strengths for

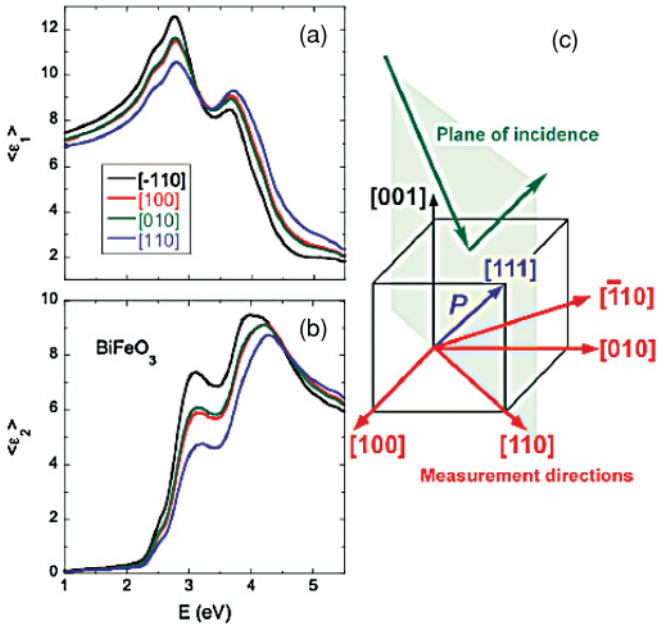

FIG. 1. (Color online) (a) Real and (b) imaginary parts of the pseudodielectric function $\langle\varepsilon\rangle$ spectra measured along four different orientations of a single-domain $BiFeO_3$ (001) crystal. The dependence of $\langle\varepsilon\rangle$ on crystallographic orientation is clearly seen. (c) A schematic depicting the SE measurement along the [110] direction.

different crystallographic directions. This effect has not been probed in previous thin-film studies.[7–9]

Even though all the spectra share common optical features, our results show a clear dependence of $\langle\varepsilon\rangle$ on the crystallographic orientation. The SE measurement is very sensitive to the projection of the ε tensor along the segment defined by the intersection of the plane of incidence and the sample surface.[14] Therefore, the strong orientation-dependence of the $\langle\varepsilon\rangle$ spectrum suggests the presence of optical anisotropy. Two orthogonal axes [100] and [010] are optically equivalent with respect to the optic axis [111], and the $\langle\varepsilon\rangle$ spectra recorded along these two axes are identical within experimental error. A schematic depicting the measurement along the [110] axis is given in Fig. 1(c). For this specific measurement geometry, the optic axis, [111], of $BiFeO_3$ (also the electric polarization vector ***P***) lies in the plane of incidence. We note that Pisarev *et al.*[15] have also observed multiple contributions in the optical structure at ~4 eV and an orientation-dependence of the $\langle\varepsilon\rangle$ spectra from their standard SE studies of bulk $BiFeO_3$, but no discussion has been made on the optical anisotropy.

For a SE measurement, the optical response of materials can be expressed mathematically using the Jones matrix:[11]

$$\begin{bmatrix} E_p \\ E_s \end{bmatrix}_{\text{out}} = \begin{bmatrix} r_{pp} & r_{sp} \\ r_{ps} & r_{ss} \end{bmatrix} \cdot \begin{bmatrix} E_p \\ E_s \end{bmatrix}_{\text{in}}. \quad (1)$$

Here, E represents an electric field, r is a reflection coefficient, and the subscripts p and s are the p and s polarization, respectively. For isotropic crystals, the off-diagonal components in the matrix vanish and the standard SE measures the ratio of the two diagonal terms r_{pp}/r_{ss}. When the principal axes of an anisotropic crystal are not aligned with the laboratory's coordinate system, however, the off-diagonal components in the Jones matrix are no longer zero and the matrix is normalized to a diagonal element to express the three measured values as[11]

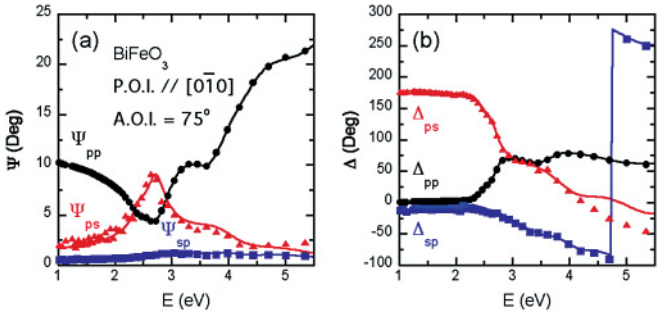

FIG. 2. (Color online) Experimental spectra (symbols) and best-fit curves (solid lines) for g-SE parameters (a) Ψ and (b) Δ. The measurements were done along [0$\bar{1}$0] direction at the incident angle of 75°.

$$\rho_{pp} = r_{pp}/r_{ss} = \tan\Psi_{pp}\exp(i\Delta_{pp}), \quad (2.1)$$

$$\rho_{ps} = r_{ps}/r_{pp} = \tan\Psi_{ps}\exp(i\Delta_{ps}), \quad (2.2)$$

$$\rho_{sp} = r_{sp}/r_{ss} = \tan\Psi_{sp}\exp(i\Delta_{sp}). \quad (2.3)$$

Hence, the six independent parameters Ψ_{pp}, Δ_{pp}, Ψ_{ps}, Δ_{ps}, Ψ_{sp}, and Δ_{sp} should be determined to describe the optical response of anisotropic crystals, whereas only two parameters Ψ and Δ are sufficient for isotropic crystals. It is the g-SE method that measures the full components of the Jones matrix.[11]

Figures 2(a) and 2(b) show experimental spectra (symbols) and the modeled curves (solid lines) for the six g-SE parameters of $BiFeO_3$ crystal measured along the [0$\bar{1}$0] direction at the incident angle of 75° as an example. Our model, consisting of a surface roughness layer and two optical functions ε_a and ε_c, shows good agreement with the experimental results, in particular for the diagonal components Ψ_{pp} and Δ_{pp}. The surface roughness, estimated to be ~10 Å, was modeled as a virtual layer whose optical functions are a 50-50 mixture of the underlying material and void using the Bruggeman effective medium approximations.[16] This procedure is based on the assumption that the absorption vanishes below the band gap. The ε_a and ε_c spectra were first obtained from the *wavelength-by-wavelength* inversion method, then parameterized by the generalized oscillator method.[17]

In order to fully analyze the uniaxial anisotropic data, it is necessary to determine two Euler angles Φ_E and Θ_E.[11] The angle Φ_E corresponds to the in-plane orientation of the crystal with respect to the plane of incidence, and Θ_E is the angle between the optic axis and the measurement surface. Φ_E is usually defined as the angle between the plane of incidence and the projection of the optic axis onto the measurement surface. Assuming the perfect (001) surface, the predicted Euler angles Φ_E and Θ_E are 135° and 55°, respectively, for experimental data shown in Figs. 2(a) and 2(b). Our best-fit Φ_E and Θ_E values were 134.4° and 61.6°, respectively. The small difference in Θ_E is in part due to the imperfect (001) surface, which was probably caused by the surface polishing.

The $\varepsilon_{a,c} = \varepsilon_{a,c1} + i\varepsilon_{a,c2}$ and $N_{a,c} = n_{a,c} + ik_{a,c}$ spectra, extracted mathematically for the tensor components along

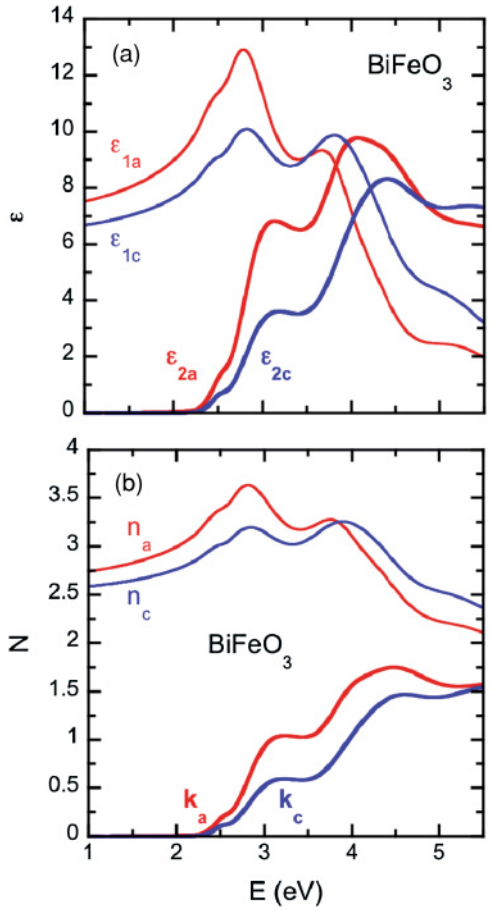

FIG. 3. (Color online) (a) Dielectric function $\varepsilon = \varepsilon_1 + i\varepsilon_2$ and (b) refractive index $N = n + ik$ spectra extracted mathematically for the tensor components along the ordinary (ε_a and N_a) and extraordinary (ε_c and N_c) principal axes of $BiFeO_3$.

the ordinary (a) and extraordinary (c) principal axes of the $BiFeO_3$ crystal, are presented in Figs. 3(a) and 3(b). Our data shown in Fig. 3(b) indicate that the $BiFeO_3$ crystal has negative uniaxial anisotropy ($n_a > n_c$) below the fundamental absorption edge ($\leqslant$2.25 eV), which is consistent with the results from a previous optical study.[18] We note that Rivera and Schmid[18] have measured the below-bandgap birefringence dispersion $dn' = n_a - n_c'$, which requires a scaling factor to obtain the birefringence $dn = n_a - n_c$. We suggest a scaling factor of about 2.2 by comparing our dn values with the dn' values reported in Ref. 18.

One of the primary objectives in solid-state spectroscopy is to determine the parameters of the optical structures shown in the ε spectrum. For $BiFeO_3$, it is known[15,19] that those optical structures are better described by the p-d and d-d charge-transfer (CT) transitions rather than the interband-transitions in semiconductors. The optical information obtained can then be used to verify the predictions made from the electronic structure calculations.

Line-shape analysis of the $d^2\varepsilon/dE^2$ spectrum is a common approach in SE study, where the ε spectrum is differentiated and smoothed numerically using the Savitzky-Golay-type[20]

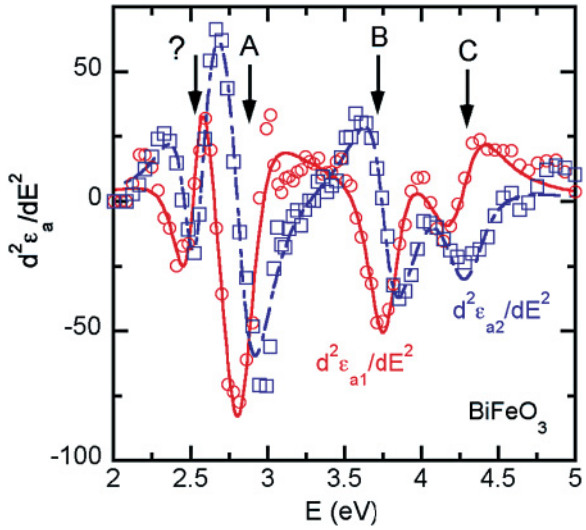

FIG. 4. (Color online) Best-fit curves for the second-energy-derivative of ε_{a1} (solid line) and ε_{a2} (dash-dotted line) of $BiFeO_3$. The open circles and open squares represent data for $d^2\varepsilon_{a1}/dE^2$ and $d^2\varepsilon_{a2}/dE^2$, respectively. Energies of each CT transition are indicated by the arrows and labeled using a notation established in a recent theoretical study.[19] The physical origin of the structure at ~2.5 eV labeled by "?" is not clear, but has been suggested as a defect-related one.

algorithms followed by least-squares fitting of standard line-shape expressions:[10]

$$\frac{d^2\varepsilon}{dE^2} = \begin{cases} n(n-1)Ae^{i\phi}(E - E_g + i\Gamma)^{n-2}, & n \neq 0, \\ Ae^{i\phi}(E - E_g + i\Gamma)^{-2}, & n = 0, \end{cases} \quad (3)$$

where A is the amplitude, E_g the threshold energy, Γ the broadening parameter, and ϕ the phase angle. The exponent n has the values of –1, $-\frac{1}{2}$, 0, and $+\frac{1}{2}$ for excitonic, one-, two-, and three-dimensional line shapes, respectively. Here, we calculated the derivative of the ε data that were obtained from the *wavelength-by-wavelength* inversion method. An appropriate level of smoothing was achieved with 11 data points to suppress noise in the derivative spectra.

Both real and imaginary parts were fitted simultaneously. Our data did not show any noticeable difference in the CT transition energies between the ε_a and ε_c spectra, so we only present the results from the ε_a spectrum here. The $d^2\varepsilon_a/dE^2$ spectra calculated from our experimental data and the corresponding best-fit curves are shown in Fig. 4. The open circles and squares represent the $d^2\varepsilon_{a1}/dE^2$ and $d^2\varepsilon_{a2}/dE^2$, respectively, whereas the solid and dash-dotted lines are the best-fit curves of the real and imaginary parts. Four line shapes

TABLE I. Charge-transfer transition energies for $BiFeO_3$ at room temperature.

CT transitions	A	B	C
Ref. 8 (thin film)	2.97		4.19
Ref. 9 (thin film)	3.2		4.3
Ref. 15 (bulk)	2.90	3.95	4.54
Ref. 19 (theory)	3.09	4.12	4.45
This work	2.83 ± 0.01	3.77 ± 0.01	4.27 ± 0.03

were used to fit the data from 2 to 5 eV, which are indicated by the arrows and labeled using a notation established in a recent first-principles calculations by Wang *et al.*[19]

The physical origin of the unidentified structure ("?") at ~2.5 eV is not clearly understood. It has been attributed to the defect states due to oxygen vacancies or collective excitations in previous SE[8,9] and theoretical[21] studies. However, a recent study[15] of $BiFeO_3$ and related iron oxides suggests that this structure has an intrinsic nature and originates from a dipole-forbidden *p-d* CT transition. A positive identification of this structure would require further theoretical investigations, which is beyond the scope of this work.

The *A*, *B*, and *C* CT structures were fit with the two-dimensional line shape ($n = 0$), whereas the unknown structure "?" was best represented by the excitonic line shape ($n = -1$). The origin of the structure *A* has been suggested as the CT transitions from either the occupied O 2*p* states to the unoccupied Fe 3*d* states or the *d-d* transition between 3*d* valence and conduction bands.[19] The structures *B* and *C* have been identified as the transitions from O 2*p* valence band to Fe 3*d* or Bi 6*p* conduction band.[19] The CT energies that we obtained are listed in Table I together with the values reported previously.[8,9,15,19] We note that many theoretical studies[19,21] calculated ε along the [100], [010], and [001] axes of the *pseudocubic* frame and reported the averaged linear $\varepsilon = (\varepsilon_{xx} + \varepsilon_{yy} + \varepsilon_{zz})/3$, which possibly resulted in the observed discrepancies in the CT energy values. It is one of our goals to provide theoreticians with the information needed to calculate ε along the ordinary and extraordinary principal axes of $BiFeO_3$.

In conclusion, we reported the ordinary and extraordinary components of the optical tensor for single-domain $BiFeO_3$ crystal determined by SE. The ε spectra exhibited three CT transition structures from 1.0 to 5.5 eV along with an unknown weak feature at 2.5 eV. The CT transition energies were obtained from the standard lineshape analysis. Our results also suggest that crystal $BiFeO_3$ has negative uniaxial optical anisotropy.

ACKNOWLEDGMENTS

This work was supported by the U.S. Department of Energy (DOE) under Contract No. DE-AC36-08GO28308. The work at Rutgers University was supported by the U.S. DOE under Grant No. DE-FG02-07ER46382.

*Author to whom correspondence should be addressed. E-mail: sukgeun.choi@nrel.gov.

[1] J. B. Neaton, C. Ederer, U. V. Waghmare, N. A. Spaldin, and K. M. Rabe, Phys. Rev. B **71**, 014113 (2005).

[2] C. Ederer and N. A. Spaldin, Phys. Rev. B **71**, 060401(R) (2005).

[3] G. Catalan and J. F. Scott, Adv. Mater. **21**, 2463 (2009).

[4] R. Palai, H. Schmid, J. F. Scott, and R. S. Katiyar, Phys. Rev. B **81**, 064110 (2010).

[5] T. Choi, S. Lee, Y. J. Choi, V. Kiryukhin, and S.-W. Cheong, Science **324**, 63 (2009).

[6] S. Y. Yang, J. Seidel, S. J. Byrnes, P. Shafer, C-H. Yang, M. D. Rossell, P. Yu, Y.-H. Chu, J. F. Scott, J. W. Ager III, L. W. Martin, and R. Ramesh, Nat. Nanotechnol. **5**, 143 (2010).

[7] J. F. Ihlefeld, N. J. Podraza, Z. K. Liu, R. C. Rai, X. Xu, T. Heeg, Y. B. Chen, J. Li, R.W. Collins, J. L. Musfeldt, X. Q. Pan, J. Schubert, R. Ramesh, and D. G. Schlom, Appl. Phys. Lett. **92**, 142908 (2008).

[8] P. Chen, N. J. Podraza, X. S. Xu, A. Melville, E. Viahos, V. Gopalan, R. Ramesh, D. G. Schlom, and J. L. Musfeldt, Appl. Phys. Lett. **96**, 131907 (2010).

[9] C. Himcinschi, I. Vrejoiu, M. Friedrich, E. Nikulina, L. Ding, C. Cobet, N. Esser, M. Alexe, D. Rafaja, and D. R. T. Zahn, J. Appl. Phys. **107**, 123524 (2010).

[10] M. Cardona, in *Modulation Spectroscopy, Suppl. 11 of Solid State Physics*, edited by F. Seitz, D. Turnbell, and H. Ehrenreich (Academic, New York, 1969).

[11] M. Schubert, in *Handbook of Ellipsometry*, edited by H. G. Tompkins and E. A. Irene (William Andrew, New York, 2005), Chap. 9.

[12] D. E. Aspnes and A. A. Studna, Phys. Rev. B **27**, 985 (1983).

[13] S. G. Choi, J. Zúñiga-Pérez, V. Muñoz-Sanjosé, A. G. Norman, C. L. Perkins, and D. H. Levi, J. Vac. Sci. Technol. B **28**, 1120 (2010).

[14] D. E. Aspnes, J. Opt. Soc. Am. **70**, 1275 (1980).

[15] R. V. Pisarev, A. S. Moskvin, A. M. Kalashnikova, and Th. Rasing, Phys. Rev. B **79**, 235128 (2009).

[16] G. E. Jellison Jr., L. A. Boatner, D. H. Lowndes, R. A. McKee, and M. Godbole, Appl. Opt. **33**, 6053 (1994).

[17] G. E. Jellison Jr., Thin Solid Films **234**, 416 (1993).

[18] J.-P. Rivera and H. Schmid, Ferroelectrics **204**, 23 (1997).

[19] H. Wang, Y. Zheng, M.-Q. Cai, H. Huang, and H. L. W. Chan, Solid State Commun. **149**, 641 (2009).

[20] A. Savitzky and M. J. E. Golay, Anal. Chem. **36**, 1627 1964).

[21] S. Ju and T.-Y. Cai, Appl. Phys. Lett. **95**, 231906 (2009).